

Design of Hexadecagon Circular Patch Antenna with DGS at Ku Band for Satellite Communications

Ketavath Kumar Naik* and Pasumarthi Amala Vijaya Sri

Abstract—The design of a hexadecagon circular patch (HDCP) antenna for dual-band operation is presented in this paper. The proposed antenna operates at two resonating frequencies 13.67 GHz, 15.28 GHz with return loss of -42.18 dB, -38.39 dB, and gain 8.01 dBi, 6.01 dBi, respectively. Impedance bandwidths of 854 MHz (13.179–14.033 GHz) and 1140 MHz (14.584–15.724 GHz) are observed for the dual bands, respectively. To produce circular polarization, the HDCP antenna is incorporated with ring and square slots on the radiating patch. The defected ground structure (DGS) is considered for enhancement of gain. Axial ratio of the proposed antenna is less than 3 dB, and $VSWR \leq 2$ for dual bands. The measured and simulated (HFSS, CST) results of the HDCP antenna are in agreement. The HDCP antenna can work at Ku band for satellite communications.

1. INTRODUCTION

The modern day communication systems require a compact antenna which provides higher gain and larger bandwidth. The conventional microstrip patch antennas have light weight, low cost and compact size which can be easily integrated in other circuit elements [1].

In the literature survey, to enhance the impedance bandwidth and achieve multiple operating frequencies some techniques have been introduced. A novel antenna design with an inverted square-shaped patch antenna [2] with a Y-shaped feeding line for broadband circularly polarized radiation patterns was considered. However, the antenna design produced a bi-directional radiation pattern with low gain of 4.6 dBi. A circular ring microstrip patch antenna [3] was designed for 4G application with bandwidths of 4% and 7% for upper and lower frequencies. The annular ring slots were loaded on the spherical-circular microstrip antenna [4] operating at 6.34 GHz frequency with impedance bandwidth of 5.98%. In [5], a compact hexagonal monopole antenna was designed to enhance the bandwidth and produced dual-band frequency, and a narrow axial ratio (1.43%) was obtained. In [6], a square ring slot antenna with an H-shaped feed line was designed for ultra-wideband (UWB) application.

The other technique is by loading band-notched filters [7], which allows antenna with small size to provide broadband characteristics. However, it exhibits asymmetric radiation patterns. Generally, polygonal patch antennas are more preferable which provide multi-frequency bands without increasing the antenna size. The irregular shapes of the patches provide irregularity in current distribution over the radiating patch, which produces limited polarization and asymmetry in radiation patterns compared to general rectangular patch antennas. The polygon-shaped patch antennas [8] provide multi-frequency and broadband operation with universal mobile telecommunications system (UMTS) terminals.

The circularly polarized patch antennas are predominantly used in wireless communication systems which mitigate the multi-path affect. The circular polarization is obtained by a circular antenna with elliptical slot patch at the center [9]. A circular patch antenna [14] and semicircular monopole antenna [15] were designed to enhance the bandwidth of the antenna. In [14], the gain of the antenna is

Received 22 September 2017, Accepted 3 November 2017, Scheduled 12 January 2018

* Corresponding author: Ketavath Kumar Naik (kumarvtr@gmail.com).

The authors are with the Antenna Research Laboratory, Department of ECE, K L University, Vaddeswaram, Guntur, AP, India.

5 dBi, and in [15], the antenna was designed with trapezoid ground plane, and a gain with 4.18 dBi was observed. A microstrip patch antenna with dodecagon (12 sided polygon) shape [10] was designed by introducing an irregular hexagonal slot on the patch, and circular polarization is generated at 2.45 GHz frequency. The DGS has been investigated and considered on the ground plane to reduce the size of the antenna and also increase the bandwidth [11].

To improve the performance of the antenna, slotting or loading techniques are considered on the ground plane. A planar structure with modifications in ground plane was considered to improve the performance of antenna with coplanar waveguide (CPW) feed arrangement to operate at UWB applications [12]. In [13], a 4×4 substrate integrated waveguide (SIW) cavity backed antenna was designed for circular polarization (CP) with a wide bandwidth at 22.75 GHz operating frequency. A hexagonal patch antenna [16], with slotted ground and parasitic elements, was designed to produce circular polarization. A microstrip UWB antenna [17] was designed, and the numerical analyses of two softwares are considered for CST, finite differential time domain (FDTD) and for HFSS, finite element method (FEM) method. More deviations are observed between CST and HFSS softwares, and good results are found with CST software.

The proposed antenna is designed with a hexadecagon-shape (16-sided polygon) on circular patch antenna. The ring slot and a square slot are loaded on the radiating patch to produce circular polarization. A diamond slot is considered at ground plane to reduce the return loss. Four rectangular slots at each corner are etched and added with a circular patch on ground plane to enhance the gain. HDCP antenna operates in dual bands with impedance bandwidths of 6.2% and 7.4%. The first operating frequency band 13.67 GHz (13.179–14.033 GHz) is operated at a space borne active sensor in EESS (Earth Exploration-Satellite Service), and the second band with operating frequency is 15.28 GHz (14.584–15.724 GHz) to work for mobile satellite service.

2. ANTENNA GEOMETRY

Figure 1 represents the geometry of the hexadecagon circular patch (HDCP) antenna, and FR4 material is used as the substrate with 4.4 of ϵ_r and 0.025 of δ . The length and width of the substrate are $L_1 \times W_1$ with 1.59 mm thickness. Top layer of the substrate is metalized with hexadecagon circular patch of side length L_3

$$L_3 = 2r_1 \sin\left(\frac{\pi}{n}\right) = 5.85 \text{ mm} \quad (1)$$

where r_1 is the radius, and n is the number of side length of the hexadecagon.

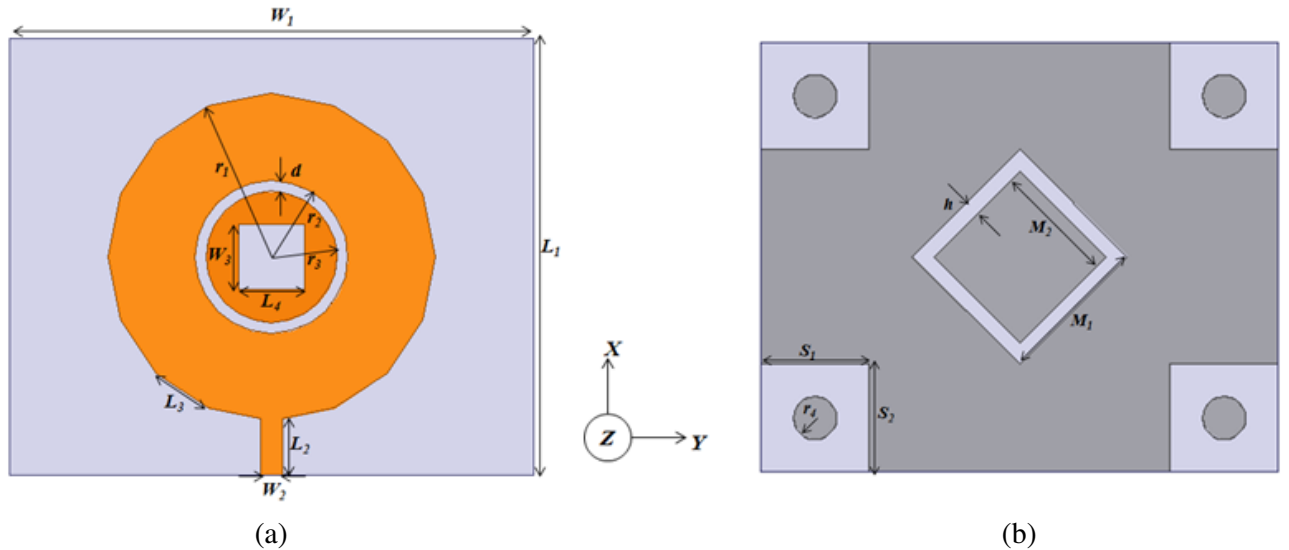


Figure 1. Geometry of the HDCP antenna, (a) radiating patch, (b) ground plane.

The HDCP antenna is designed with an annular ring slot and square slot on the radiating patch, shown in Fig. 1(a). The thickness of the annular ring slot is d with r_2 and r_3 as inner and outer ring radii. The dimension of the square slot is $L_4 \times W_3$. The optimized variables of the HDCP antenna are listed in Table 1.

Table 1. Optimized values of HDCP antenna.

Variables	Values (mm)	Variables	Values (mm)
$L1$	40	h	2
$W1$	48	d	1
$L2$	5	$r1$	16
$W2$	2	$r2$	7
$L3$	5.85	$r3$	6
$W3$	6	$r4$	2
$L4$	6	$S1$	10
$M1$	14.14	$S2$	10
$M2$	11.31	n	16

Figure 1(b) shows the defected ground structure. The diamond slot at the center on the ground plane is etched with external side length M_1 , internal side length M_2 and slot thickness h . The four corners of the ground plane are etched with four square slots with dimensions $S_1 \times S_2$. The ground plane of the antenna is added with four circular patches at the center of the four square slots with radius r_4 as shown in Fig. 1(b). A feed line patch is added to the HDCP antenna with dimensions $L_2 \times W_2$. In order to improve the bandwidth of the HDPC antenna, the diamond slot and the four square slots at each corner of the ground plane are considered. The ring slots on radiating patch and circular patches of the ground plane produce the polarization.

3. DESIGN

To design the hexadecagon circular patch (HDCP) antenna, consider the first circular patch antenna design, as it is closely related to HDCP design [1, 10, 16]. The resonant frequency of the circular patch antenna can be derived with zeroth-order approximation of the Bessel functions [1]. The resonant frequency of circular patch is given by [1, 10] as

$$f_r = \frac{8.794}{r_e \sqrt{\epsilon_r}} \tag{2}$$

where, f_r is the resonant frequency of the patch, ϵ_r the relative permittivity of the substrate, and r_e the effective radius of the circular patch given by [1]

$$r_e = r_1 \left[1 + \frac{2h}{\pi r_1 \epsilon_r} \left\{ \ln \left(\frac{r_1}{2h} \right) + (1.41\epsilon_r + 1.77) + \frac{h}{r_1} (0.268\epsilon_r + 1.65) \right\} \right]^{1/2} \tag{3}$$

where, r_1 is the radius of the circular patch and h the height of the substrate.

Equation (2) can be applied to design a hexadecagon circular patch antenna by relating the areas of the circular and the hexadecagon circular patches as shown in Equation (4) by [16].

$$\pi r_e^2 = 20.65 L_3^2 \tag{4}$$

where L_3 is the side length of the hexadecagon circular patch.

4. RESULTS AND DISCUSSIONS

The analysis has been carried out by computer simulation technology (CST) and high frequency structure simulator (HFSS) simulators for HDCP antenna model. Photographs of the HDCP antenna are presents in Fig. 2.

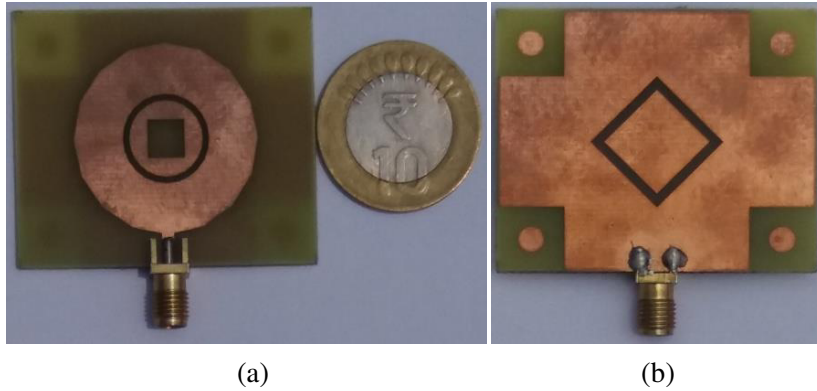


Figure 2. Prototype of fabricated HDCP antenna, (a) front view, (b) bottom view.

It is composed of a $50\ \Omega$ microstrip feed line. The measurements are carried out in the antenna testing facility laboratory with an anechoic chamber and vector network analyzer (ZNB-20, R&S), shown in Fig. 3.

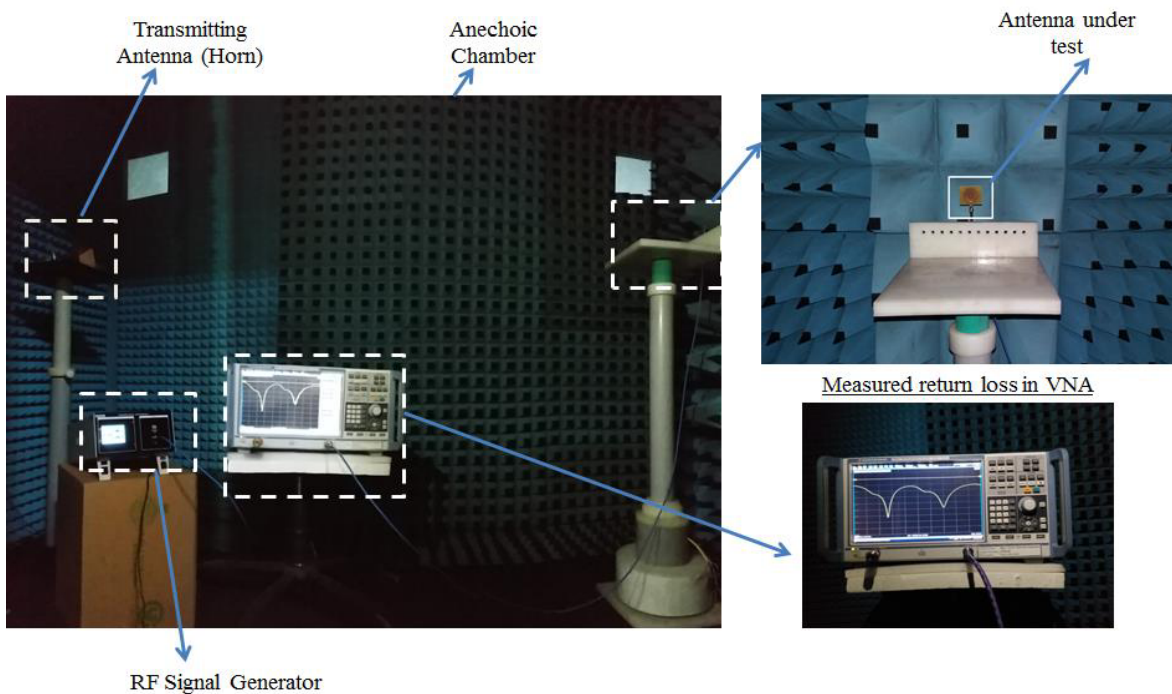


Figure 3. Photograph of HDCP antenna testing setup.

The comparison of basic circular patch antenna and the proposed HDCP antenna is shown in Fig. 4. It is observed that the circular patch has two operating frequencies 13.5 GHz and 15.3 GHz with return losses $-16.73\ \text{dB}$ and $-17.34\ \text{dB}$. The gains of the circular patch antenna are 3.53 dBi and 4.28 dBi at two frequencies, respectively.

The operating frequencies of the proposed HDCP antenna are 13.67 GHz and 15.28 GHz with the return losses $-42.18\ \text{dB}$ and $-38.39\ \text{dB}$. The gains are 8.01 dBi and 6.01 dBi, respectively, which are higher than the circular patch antenna. The analysis of HDCP antenna shows good result compared to basic circular patch antenna.

The proposed HDCP antenna exhibits two operating frequency bands for HFSS and CST

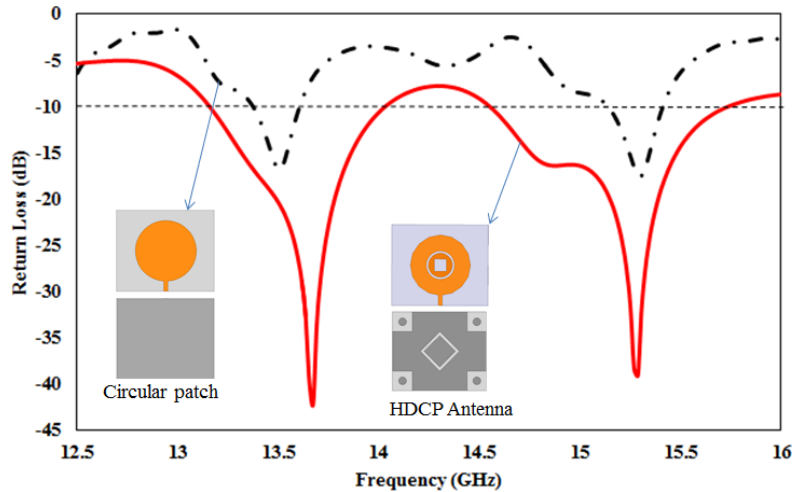


Figure 4. Comparison of circle and hexadecagon circular patch antenna.

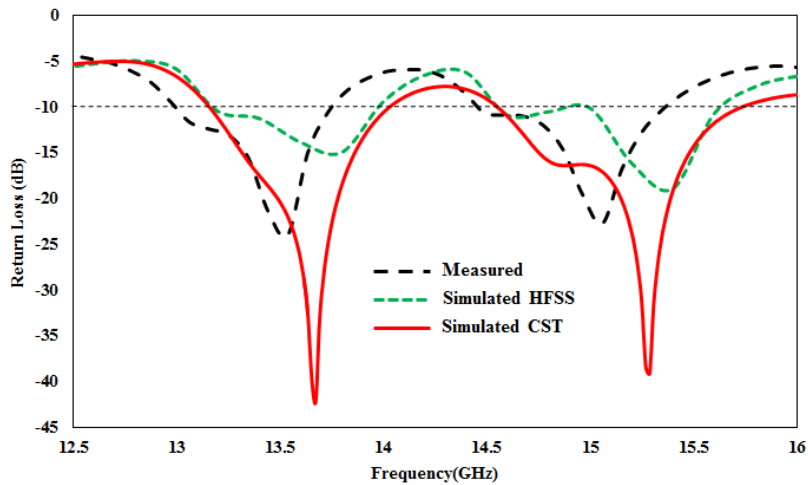


Figure 5. Return loss (S_{11} dB) for the HDCP antenna.

simulations. The measurement has been carried out, and comparison of return loss plot (S_{11} dB) is shown in Fig. 5. In Table 2, the comparison data are presented for two operating bands for HFSS, CST and measured values with deviations. The CST simulation return loss values are observed closely following the measured return loss values as compared with HFSS simulation values. At 13.67 GHz frequency band 130 MHz deviation and 15.28 GHz band 140 MHz deviation are observed for CST simulations with measured values. The deviations of simulated HFSS and measured values 360 MHz and 440 MHz at two operating frequencies are observed. In [17], similar deviations are observed for CST and HFSS software with measured values due to the numerical analysis. The frequency shift between simulated CST and measured values is minimum and acceptable, and this deviation is due to parasitic effects.

So, the simulation analysis has been carried out with CST simulation tool. The resonant frequencies are found at 13.67 GHz and 15.28 GHz, and the impedance bandwidths of 854 MHz (13.179 GHz–14.033 GHz) and 1140 MHz (14.584 GHz–15.724 GHz) are observed respectively for satellite communication applications in Ku band. The return losses for the two resonant frequencies are found -42 dB and -39 dB respectively of the dual bands. The operating frequencies of the measured values are reported in Table 2 of proposed HDCP antenna with the return losses -23.91 dB, -22.71 dB respectively of the dual bands. The deviations of return loss for CST simulation and measured values are observed 18.27 dB and 15.68 dB respectively of the dual bands.

Table 2. Comparison for simulated and measured results of proposed HDCP antenna for two operating frequencies.

Parameter	Simulated HFSS (GHz)	Simulated CST (GHz)	Measured (GHz)	Deviations in HFSS Vs Measured (MHz)	Deviations in CST Vs Measured (MHz)
Operating Frequency	13.9	13.67	13.54	360	130
	15.5	15.28	15.06	440	140

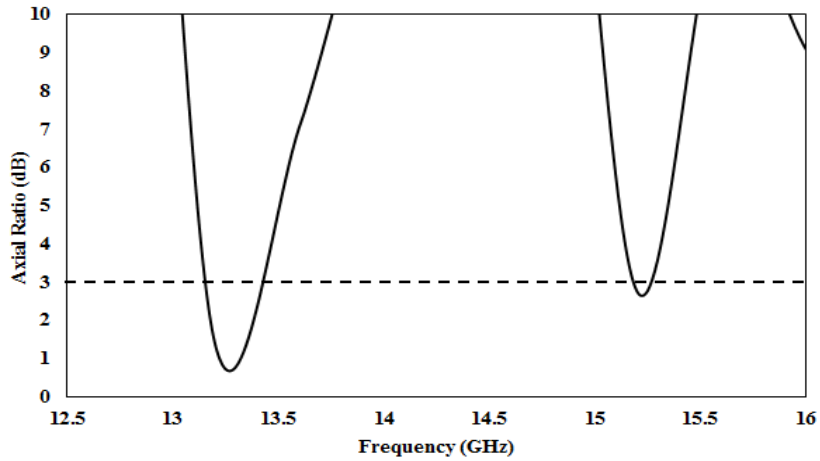


Figure 6. Axial ratio of the HDCP antenna.

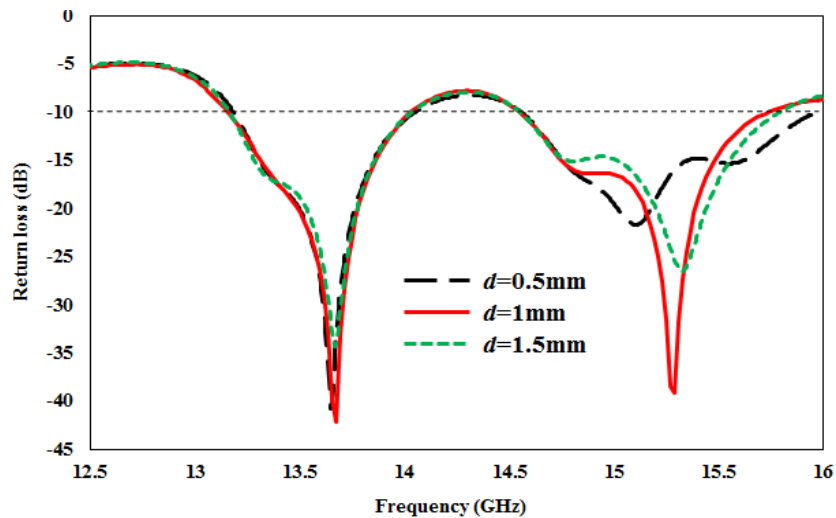


Figure 7. Return loss of HDCP antenna by varying d variable.

The axial ratio (AR) of the HDCP antenna is presents in Fig. 6 with $AR < 3$ dB for dual bands with first bandwidth of 335 MHz (13.4 GHz–13.735 GHz) and second bandwidth of 550 MHz (15.25 GHz–15.8 GHz).

The parametric analysis has been carried out on the proposed HDCP antenna by varying the dimensions of annular ring slot width and square slot width of radiating patch antenna. The annular ring slot width d is varies at 0.5 mm, 1 mm, and 1.5 mm of HDCP antenna, shown in Fig. 7 with respect to return loss and frequency.

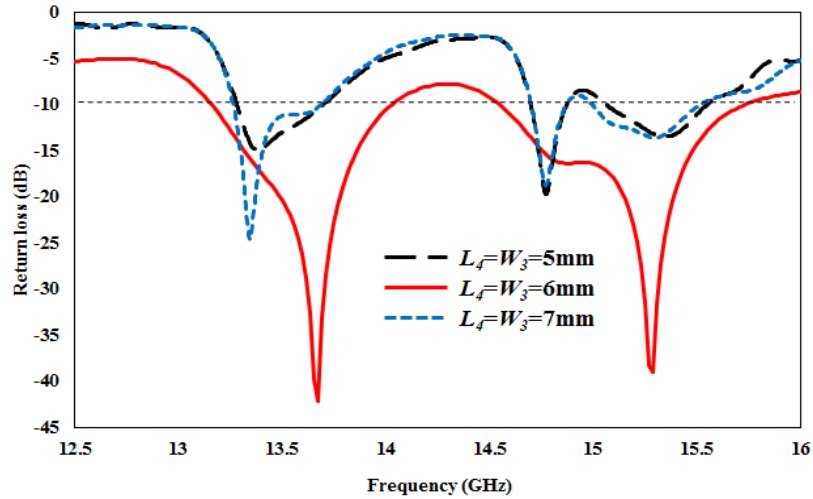


Figure 8. Return loss by varying L_4 and W_3 variables.

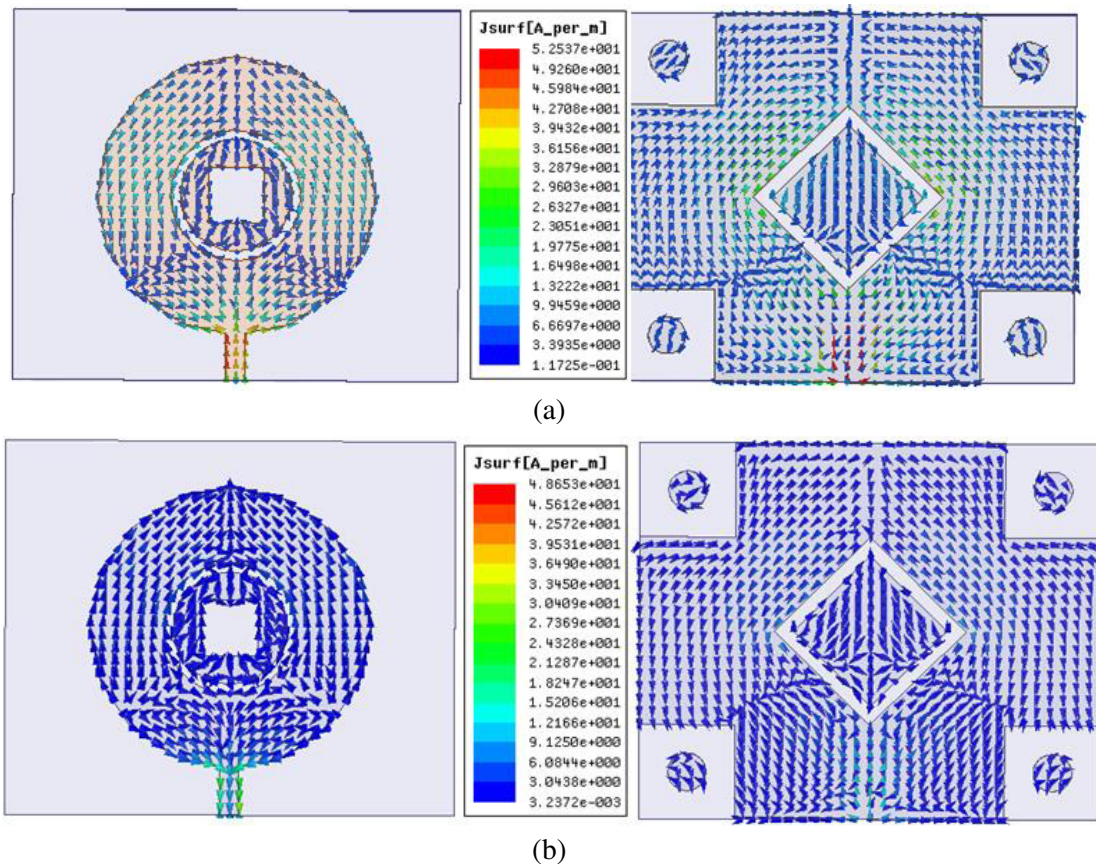


Figure 9. Current distribution of HDCP antenna at frequency, (a) 13.67 GHz, (b) 15.28 GHz.

Figure 8 shows the S_{11} (dB) plot of the HDCP antenna by varying the square slot dimensions ($L_4 = W_3$) as 5 mm, 6 mm and 7 mm. However, the ring slot dimensions 1 mm and square slot dimensions 6 mm of the proposed antenna model show the optimum return loss.

The surface current distribution of HDCP antenna is presented in Fig. 9. The circular polarization of the antenna is observed at the circular ring slot on the radiating patch and the circular patches on

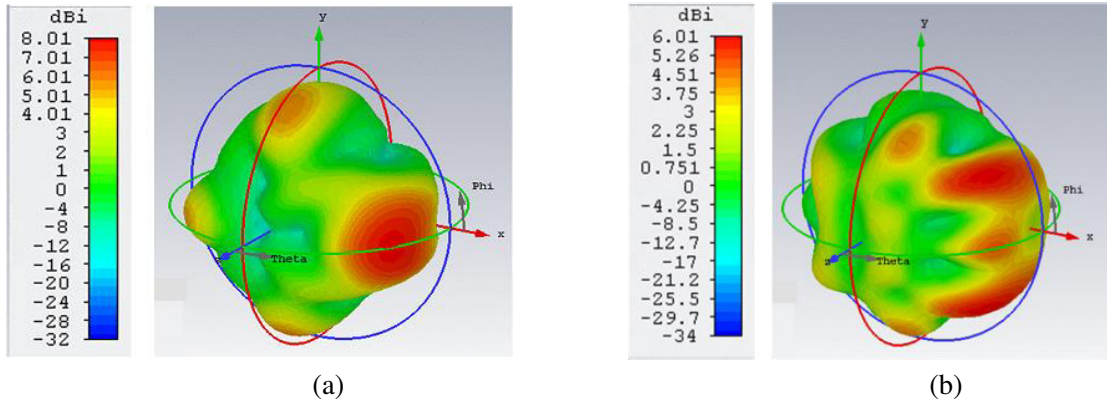


Figure 10. Gain plot of the HDCP antenna at frequency, (a) 13.67 GHz, (b) 15.28 GHz.

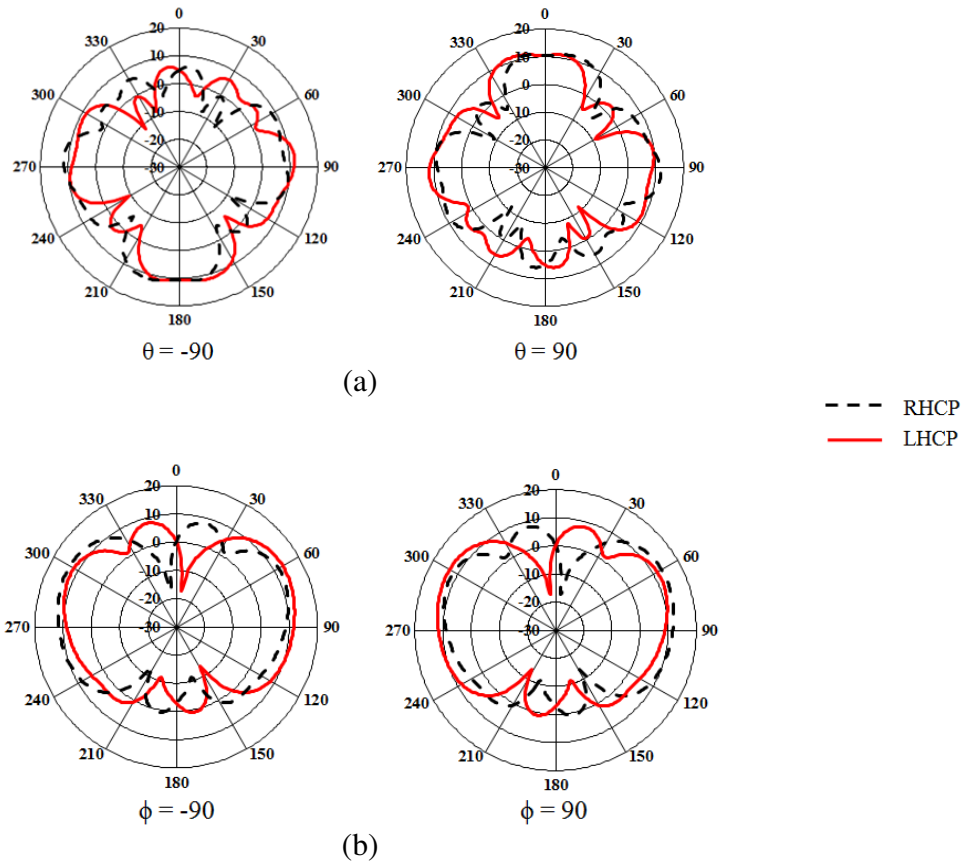


Figure 11. Radiation patterns of HDCP antenna for 13.67 GHz, (a) $\theta = -90^\circ$, $\theta = 90^\circ$, (b) $\phi = -90^\circ$, $\phi = 90^\circ$.

the ground plane. The 3D gain plot of the proposed HDCP antenna is shown in Fig. 10 for 13.67 GHz and 15.28 GHz frequencies.

The radiation patterns of the HDCP antenna with left-hand circular polarization (LHCP) and right-hand circular polarization (RHCP) are shown in Fig. 11 and Fig. 12 for the two operating frequency bands, respectively. To avoid the multipath fading in satellite communication, the proposed antenna is used either in LHCP or RHCP polarization. From the observations, the plots are generated with equal magnitudes in LHCP and RHCP but a phase shift of 180 for different values of elevation (θ),

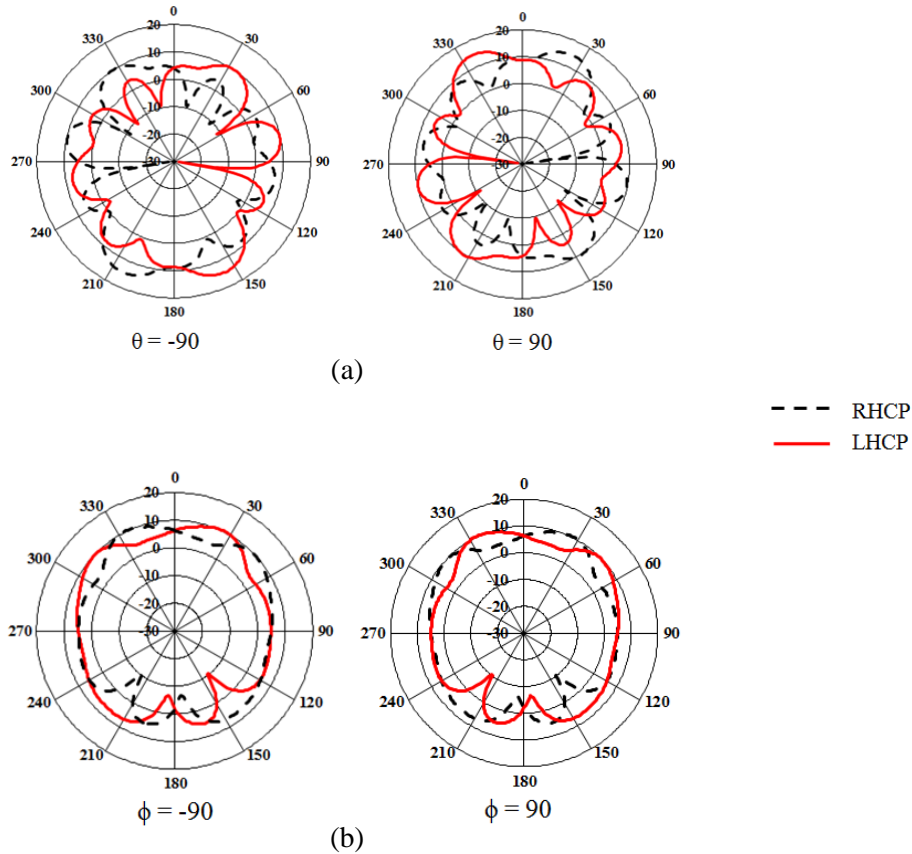


Figure 12. Radiation patterns of HDCP antenna for 15.28 GHz, (a) $\theta = -90^\circ$, $\theta = 90^\circ$, (b) $\phi = -90^\circ$, $\phi = 90^\circ$.

Table 3. Comparison of existing antenna models to proposed HDCP antenna.

Ref. No.	Antenna Size (mm ³)	Material	No. of bands	Operating Frequency (GHz)	Gain (dBi)	Application
[5]	30 × 30 × 1.57	RT5880 ($\epsilon_r = 2.2$)	2	6.65 7.33	2.8 3.1	UWB
[8]	53 × 38.5 × 5	FR-4 ($\epsilon_r = 4.4$)	2	2.44 5.25	2.1 -	UWB
[9]	50 × 50 × 1.6	FR-4 ($\epsilon_r = 4.4$)	1	2.45	3.85	WLAN
[10]	50 × 50 × 1.6	FR-4 ($\epsilon_r = 4.4$)	1	2.45	4.82	RFID
[11]	60.4 × 99.8 × 1.524	R04003 ($\epsilon_r = 3.38$)	1	1.480	-	-
[12]	25 × 25 × 1.6	FR4 ($\epsilon_r = 4.4$)	3	3.03 6.11 11.78	1.05 1.15 1.3	UWB
[13]	50 × 50 × 5.3	RT5880 ($\epsilon_r = 2.2$)	1	25	7.8	-
Proposed antenna	40 × 48 × 1.59	FR4 ($\epsilon_r = 4.4$)	2	13.67 15.28	8.01 6.01	Satellite Communication

azimuth (ϕ) angles in two operating bands. The radiation patterns are observed with 180 out of phase for the two resonating frequencies. The comparison of existing antenna models to the proposed HDCP antenna is tabulated in Table 3 in terms of size, material, number of bands, operating frequency, gain, and applications.

Comparing the previous research antenna models, the proposed HDCP antenna has good performance characteristics, small size and very high gain.

5. CONCLUSION

The design of a hexadecagon circular patch (HDCP) antenna with DGS is presented in this paper. The HDCP antenna operates at 13.67 GHz, 15.28 GHz with return losses -42.18 dB, -38.39 dB, and gains 8.01 dBi, 6.01 dBi, respectively. The antenna structure provides design flexibility with desired gain, VSWR ≤ 2 and axial ratio < 3 dB. The proposed antenna avoids multipath fading in satellite communications because it operates in LHCP and RHCP at Ku band.

ACKNOWLEDGMENT

This work was supported by the SERB, Department of Science and Technology (DST), New Delhi, India. (Grant No. 1: SB/FTP/ETA-0179/2014, Grant No. 2: EEQ/2016/000754.)

REFERENCES

1. Garg, R., P. Bhartia, I. Bahl, and A. Ittipiboon, *Microstrip Antenna Design Handbook*, Artech House, London, 2001.
2. Shen, J., C. Lu, W. Cao, J. Yang, and M. Li, "A novel bidirectional antenna with broadband circularly polarized radiation in X-band," *IEEE Antennas Wireless Propag. Lett.*, Vol. 13, 7–10, 2015.
3. Abdelaal, M. A. and H. H. M. Ghouz, "New compact circular ring microstrip patch antennas," *Progress In Electromagnetic Research C*, Vol. 46, 135–143, 2014.
4. Chen, H. T., H. D. Chen, and Y. T. Cheng, "Full-wave analysis of the annular-ring loaded spherical-circular microstrip antenna," *IEEE Trans. Antennas Propag.*, Vol. 45, 1581–1583, Nov. 1997.
5. Shaalan, A. A. M. and M. I. Ramadan, "Design of a compact hexagonal monopole antenna for ultra-wideband application," *J. Infrared Milli. Terahz. Waves*, Vol. 31, 958–968, 2010.
6. Sadat, S., M. Houshmand, and M. Roshandel, "Design of microstrip square ring slot antenna filled by an H-shaped slot for UWB applications," *Progress In Electromagnetic Research*, Vol. 70, 191–198, 2007.
7. Yin, X.-C., C.-L. Ruan, C.-Y. Ding, and J.-H. Chu, "A compact ultra-wideband microstrip antenna with multiple notches," *Progress In Electromagnetics Research*, Vol. 84, 321–332, 2008.
8. Manzini, M., A. Alù, F. Bilotti, and L. Vegni, "Polygonal patch antennas for wireless communications," *IEEE Trans. Vehicular Technology*, Vol. 53, 1434–1440, 2004.
9. Maddi, S., A. Cidronali, and G. Manes, "A new design method for single-feed circular polarization microstrip antenna with an arbitrary impedance matching condition," *IEEE Trans. Antennas Propag.*, Vol. 59, 379–389, 2011.
10. Prakash, K. C., S. Mathew, R. Anitha, P. V. Vinesh, M. P. Jayakrishnan, P. Mohanan, and K. Vasudevan, "Circularly polarized dodecagonal patch antenna with polygonal slot for RFID applications," *Progress In Electromagnetics Research C*, Vol. 61, 9–15, 2016.
11. Chiang, K. H. and K. W. Tam, "Microstrip monopole antenna with enhanced bandwidth using defected ground structure," *IEEE Antennas Wireless Propag. Lett.*, Vol. 7, 532–535, 2008.
12. Gautam, A. K., S. Yadav, and B. K. Kanaujia, "A CPW-fed compact UWB microstrip antenna," *IEEE Antennas Wireless Propag. Lett.*, Vol. 12, 151–154, 2013.
13. Lang, Y., S. W. Qu, and J. X. Chen, "Wideband circularly polarized substrate integrated cavity-backed antenna array," *IEEE Antennas Wireless Propag. Lett.*, Vol. 13, 1513–1516, 2014.

14. Singh, R. K. and D. Pujara, "Design of an UWB (2.1–38.6 GHz) circular microstrip antenna," *Wiley — Microwave and Optical Technology Letters*, 2762–2767, DOI: 10.1002/mop.30813, Apr. 2017.
15. Samsuzzaman, M. and M. T. Islam, "A semicircular shaped super wideband patch antenna with high bandwidth dimension ratio," *Wiley — Microwave and Optical Technology Letters*, Vol. 57, 445–452, Feb. 2015.
16. Kushwaha, N. and R. Kumar, "Design of slotted ground hexagonal microstrip patch antenna and gain improvement with FSS screen," *Progress In Electromagnetics Research B*, Vol. 51, 177–199, 2013.
17. Lim, K.-S., M. Nagalingam, and C.-P. Ta, "Design and construction of microstrip UWB antenna with time domain analysis," *Progress In Electromagnetics Research M*, Vol. 3, 153–164, 2008.